Mesoporous Carbons from Poly(acrylonitrile)-*b*-poly(ϵ-caprolactone) Block Copolymers

Rong-Ming Ho,*,† Tzu-Chung Wang,† Chu-Chieh Lin,*,‡ and Te-Liang Yu‡

Department of Chemical Engineering, National Tsing Hua University, Hsinchu 30013, Taiwan, R.O.C., and Department of Chemistry, National Chung Hsing University, Taichung 40227, Taiwan, R.O.C.

Received December 6, 2006; Revised Manuscript Received January 31, 2007

ABSTRACT: A series of degradable block copolymers, poly(acrylonitrile)-*b*-poly(ϵ-caprolactone) (PAN−PCL), have been synthesized by sequential living polymerization in this study. Well-defined, microphase-separated PAN−PCL microdomains can be efficiently achieved in the bulk by using appropriate solvents. The microphase-separated lamellar samples were then used as templates to produce mesoporous carbons at which large amounts of porous texture in carbonized PAN matrix were formed after degradation of PCL due to randomly oriented lamellar texture (namely, interconnection of PCL microdomains). The thermal profiles for efficient stabilization were examined by differential scanning calorimetry and thermogravimetric analyses as well as Fourier transform infrared spectroscopy. Consequently, mesoporous carbon materials might be prepared as evidenced by transmission electron microscopy, field emission scanning electron microscopy, and small-angle X-ray scattering. The formation of carbonized materials was identified in accordance with the presence of carbon diffractions by wide-angle X-ray diffraction. In contrast to the thermal stability of the carbonization of PAN homopolymers, it is noted that the carbonization procedure can be achieved in the PAN−PCL system regardless of the stretching process (that is an essential process to improve the thermal stability of PAN carbonization). We speculate that this unique feature for the carbonization of PAN copolymers might be attributed to the stretched chains of PAN under nanoscale confined environment.

Introduction

Mesoporous carbon materials with high areas, large pore volume, and good chemical resistance have received extensive attention due to their potential applications as water and air purification, gas separation, catalysis, chromatography, and hydrogen storage systems.[1,2] One of the most common synthetic techniques used to produce mesoporous carbons is based on the templation of carbon precursor such as cyclodextrin,[3] divinylbenzene,[4] furfuryl alcohol,[5,6] phenol, resorcinol, formaldehyde,[7,8] pitch, sucrose,[9] and poly(acrylonitrile) (PAN)[10,11] into a regular inorganic template such as zeolite[12] or mesoporous silica.[6,13−15] Carbonization of the precursors and subsequent removal of the inorganic templates result in mesoporous carbons with templated pore structure. So far, many researchers have prepared novel mesoporous carbons with this technique by using a variety of inorganic mesoporous templates. Similar to other carbon materials, it is expected that these mesoporous carbons should exhibit widely different physicochemical properties depending on the detailed structure of the frameworks. However, the synthesis of such mesoporous carbons with pore regularity was hitherto limited to carbon networks with an amorphous-carbon-like nature.

Recently, using microphase-separated PAN block copolymers as template for mesoporous carbons has been extensively studied by many researchers. PAN is a famous carbonization precursor. Carbonization of PAN precursors can be achieved by stabilization (at 200−300 °C in the presence of air) and carbonization (at 800−1000 °C in inert environment) in sequence. Graphitization of carbonized fibers is usually obtained at a higher temperature, 2500−3000 °C, to eliminate the original oxygen and hydrogen so as to increase the percentage of carbon to over 99%.[16−21] For templation, PAN block with sacrificial blocks (i.e., poly(*n*-butyl acrylate) (PBA),[22−24] poly(acrylic acid) (PAA),[25] poly(styrene) (PS),[26] and poly(ethylene oxide) (PEO)[27]) copolymer systems have been synthesized. Long-range ordered thin-film textures of PAN−PBA block copolymers, synthesized by Matyjaszewski and co-workers, can be prepared by spin-casting[22,23] or zone-casting.[24] The sacrificial block can be removed by volatilization, and then oriented block copolymer thin films were converted to nanostructured carbon thin films after carbonization of PAN component. Also, the block copolymer system PS−PAN, which was synthesized by Russell and co-workers, was used to prove this strategy of manufacturing nanostructured carbons.[26] PAN−PAA block copolymers have also been synthesized where carbon precursor, PAN, and water-soluble sacrificial block, PAA, served as core and corona in a mixture of DMF and water to form specific shell cross-linked knedels (SCKs).[25] More recently, an interesting approach by combining the strategies of the synthesis of nanostructured carbons from microphase-separated block copolymers and the synthesis of mesoporous carbons through inverse replication of mesoporous silica, proposed by Matyjaszewski and co-workers, gave rise to form mesoporous carbons and mesoporous silica templates from PAN−PEO block copolymers.[27] Also, another strategy for the manufacturing of mesoporous carbons was demonstrated by Dai and co-workers,[28] where a microphase-separated and well-oriented PS−P4VP/resorcinol template was polymerized within a formaldehyde as a highly cross-linked resorcinol−formaldehyde resin (RFR), and subsequent carbonization led to an ordered mesoporous carbon film.

The objective of this study is the manufacture of mesoporous carbons via carbonization of microphase-separated PAN-containing block copolymers with degradable character. Block copolymers containing aliphatic polyesters draw extensive

* Corresponding authors: R.-M. Ho: Tel 886-3-5738349; Fax 886-3-5715408; e-mail rmho@mx.nthu.edu.tw. C.-C. Lin: Tel 886-4-22840411 ext 718; Fax 886-4-22862547.

† National Tsing Hua University.

‡ National Chung Hsing University.

10.1021/ma062798y CCC: $37.00
Published on Web 03/17/2007

Scheme 1. Synthetic Route of PAN−PCL Block Copolymers

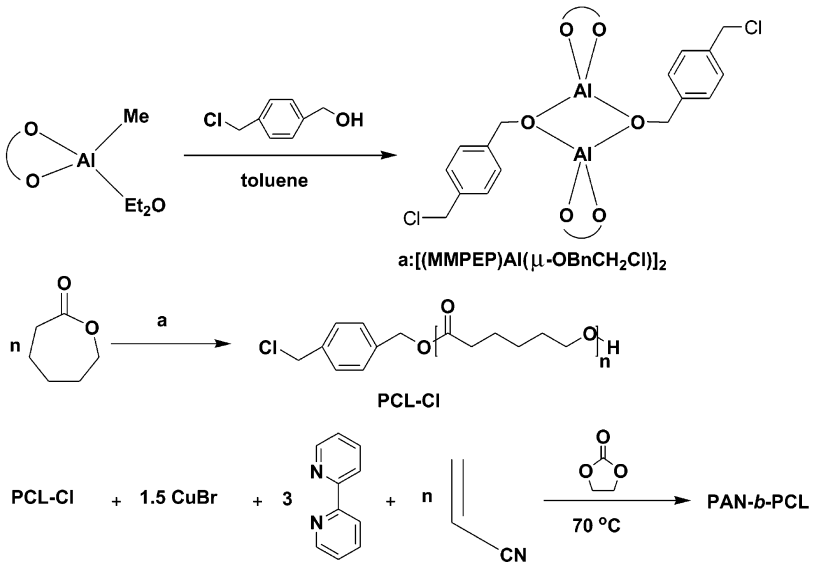

attention in the preparation of mesoporous polymers attributed to the ease degradation of ester groups.[29−33] Herein, we report a synthetic strategy to fabricate mesoporous carbon materials with graphite-like network structure through self-assembled block copolymers in which the carbon precursor (PAN) is preorganized into well-defined nanostructures (e.g., cubic, cylinder, lamellae) induced by the presence of degradable block (i.e., poly(ϵ-caprolactone) (PCL)) which could be removed by pyrolysis or hydrolysis. Also, we found that the carbonization procedure can be achieved in the PAN−PCL system regardless of the stretching process (that is an essential process to improve the thermal stability of PAN carbonization). Consequently, this approach may provide a satisfactory addition to the methods for the manufacturing of mesoporous carbons from PAN-containing block copolymers and a new way for PAN carbonization by taking advantage of microphase separation.

Experimental Section

Synthesis of PAN−PCL Block Copolymers. A series of poly(acrylonitrile)-*b*-poly(ϵ-caprolactone) (PAN−PCL) diblock copolymers were prepared by using two-step polymerization sequence as shown in Scheme 1. $[(MMPEP)Al(\mu\text{-}OBnCH_2Cl)]_2$ was prepared from the reaction of $[(MMPEP)Al(CH_3)(OEt_2)]_2$ with the stoichiometric amount of *p*-(methyl chloride)benzyl alcohol in toluene.[34,35] Ring-opening polymerization of ϵ-caprolactone using $[(MMPEP)Al(\mu\text{-}OBnCH_2Cl)]_2$ in toluene solution resulted in a *p*-(chloromethyl) benzyl ester end-functionalized poly(ϵ-caprolactone), a macroinitiator for ATRP of acrylonitrile, at 50 °C for 1 h in nitrogen atmosphere. PAN−PCL was then prepared by the polymerization of acrylonitrile according to ATRP method, developed by Matyjaszewski and co-workers,[22−24] using CuBr/2,2-bipyridine as catalyst and poly(ϵ-caprolactone) as macroinitiator in ethylene carbonate solution at 70 °C. The copolymers with different volume ratios can be synthesized by mixing different amounts of PCL and acrylonitrile.

Gel permeation chromatography (GPC) measurements were performed on a Hitachi L-7100 system equipped with a differential Bischoff 8120 RI detector using THF (HPLC grade) as eluent for PCL homopolymers or a Postnova PN1122 solvent delivery system equipped with a RI detector PN3110 using DMF (HPLC grade) as eluent for PAN−PCL block copolymers. Molecular weight and molecular weight distribution were calculated using polystyrene as standard. The number-average molecular weight (M_n) of *p*-(methyl chloride) benzyl ester end-functionalized PCL homopolymer and polydispersity (PDI) of PAN−PCL block copolymer were obtained by GPC analysis. The molecular weights of PCL and PAN blocks were measured by ^{1}H NMR analysis using D-DMSO (HPLC grade) as eluent for PAN−PCL block copolymers on a Varian Mercury-400 (400 MHz) spectrometer with chemical shifts given in ppm from the internal TMS. On the basis of molecular weight and volume ratio, these PAN−PCLs, AN05CL03 ($f_{PAN^v} = 0.6$, PDI = 1.16) and AN03CL05 ($f_{PAN^v} = 0.33$, PDI = 1.22), are designated as AN*x*-CL*y* ($f_{PAN^v} = z$), where *x* and *y* represent the symbol of molecular weight (kg/mol) for PAN and PCL blocks measured by NMR, respectively, and *z* indicates the volume fraction of PAN calculated by assuming densities of PAN and PCL are 1.22 and 1.08 g/cm^3.

Sample Preparation. Bulk samples of block copolymers were prepared by solution-casting from *N*,*N*-dimethylformamide ($HCON(CH_3)_2$, DMF) solution (100 mg/mL of PAN−PCL) at temperature above the melting temperature of PCL (i.e., 70 °C) for 3 days. After solution casting, sample was annealed at 160 °C for 12 h in vacuum oven.

Differential Scanning Calorimetry (DSC). DSC experiments were carried out in a Perkin-Elmer DSC 7 for the measurements of thermal behavior of PAN−PCL block copolymers and PCL homopolymers. The thermal properties of examined samples such as melting temperature, glass transition temperature, and heat of melting were obtained by heating at 10 °C/min after cooling by 10 °C/min from a temperature higher than the glass transition of PAN (i.e., 180 °C) in nitrogen. In the case of stabilization analysis, the thermograms of PAN−PCLs and PAN homopolymers were obtained on heating at 10 °C/min from ambient conditions in air atmosphere.

Transmission Electron Microscopy (TEM). Microsections of solution-cast PAN−PCL bulk samples having thickness about 40 nm were obtained by ultra-microtomy using a Reichert Ultracut microtome. Bright field TEM images were obtained by mass−thickness contrast on a JEOL TEM-1200x transmission electron microscopy, at an accelerating voltage of 120 kV. Staining was accomplished by exposing the samples to the vapor of a 4% aqueous RuO_4 solution for 3 h. Bright field images of mass−thickness contrast were obtained from the stained samples. By contrast, the microsections of thermally degraded samples were directly examined by TEM without staining, and ED experiments for the thin films were also carried out. However, the microsections of carbonized samples were hard to be performed due to the dramatically increasing rigidity upon carbonization.

Small-Angle X-ray Scattering (SAXS) and Wide-Angle X-ray Diffraction (WAXD). SAXS experiments were conducted at the synchrotron X-ray beamline X27C at the National Synchrotron Light Source in Brookhaven National Laboratory. The wavelength of the X-ray beam was 0.1371 nm. The zero pixel of the SAXS

patter was calibrated using silver behenate, with the first-order scattering vector q^* ($q^* = 4\pi\lambda^{-1} \sin\theta$, where 2θ is the scattering angle) being 1.076 nm^{-1}. Time-resolved SAXS experiments were carried out in a heating chamber with step temperature increasing.

A Siemens D5000 1.2 kW tube X-ray generator (Cu Kα radiation) with a diffractometer was used for wide-angle X-ray diffraction (WAXD) powder experiments. The scanning 2θ angle ranged between 5° and 40° with a step scanning of 0.05° for 3 s. The diffraction peak positions and widths observed from WAXD experiments were carefully calibrated with silicon crystals with known crystal size.

Thermogravimetric Analysis (TGA). Thermal stability of synthesized samples was assessed with a Perkin-Elmer Pyris1 TGA. The samples were first ramped to 50 °C and then heated by 10 °C/min to 750 °C. Measurements were conducted in air. The weight loss rate was obtained from the differential results of the weight loss profile.

Fourier Transform Infrared Spectroscopy (FTIR). The stabilization procedure in PAN−PCL was monitored with an FTIR spectrometer (Perkin-Elmer 842 IR spectrometer). IR measurements were made on the KBr disks (1 mg sample with 200 mg KBr). The FTIR was used at a resolution of 0.5 cm^{-1} to detect the structural changes upon stabilization reaction.

Field Emission Scanning Electron Microscopy (FESEM). FESEM observations were performed on a JEOL JSM-6700F using accelerating voltages of 0.5−1 keV. Samples were examined on PAN−PCL microsections deposited onto silicon wafers having a silicon oxide layer. The samples were mounted to brass shims using carbon adhesive and then sputter-coated with 2−3 nm of platinum (the platinum coating thickness was estimated from a calculated deposition rate and experimental deposition time).

Mesoporous Scaffold Preparation by Pyrolysis. Bulk samples of PAN−PCL were heated at 230 °C for 20 h in air atmosphere for stabilization reaction on a hot stage (Instec STC200). After air cooling to room temperature, the stabilized samples were then heated by 1 °C/min to 800 °C under vacuum to thermally degrade PCL component and also carbonize the stabilized samples.

Mesoporous Scaffold Preparation by Hydrolysis. Bulk samples of PAN−PCL were heated at 230 °C for 20 h in air atmosphere for stabilization reaction on a hot stage (Instec STC200). The stabilized samples were then hydrolyzed by using different base solutions including a sodium hydroxide solution (by dissolving 2 g of sodium hydroxide in a 25 mL of 40/60 (by volume) solution of methanol/water)[29] and a potassium hydroxide solution (by dissolving 500 mg of potassium hydroxide and 50 mg of cetyltrimethylammonium bromide (CETAB) in a 12 mL of 50/50 (by volume) solution of methanol/water while CETAB is incorporated to improve the surface wetting and etching uniformity.[36] In the case of sodium hydroxide solution, the hydrolysis rate for PCL component was found to be extremely slow (only a trace amount of PCL hydrolysis after 2 week execution). By contrast, significant PCL hydrolysis occurred by using potassium hydroxide solution at which complete degeneration was achieved after 2 day execution.

Results and Discussion

Microphase-Separated Morphology. Since PAN−PCL is a semicrystalline block copolymer, to realize how crystallization affects the microphase-separated morphology is essential. To examine the mutual interaction between crystallization and microphase separation, the thermal behavior of synthesized PAN−PCLs were studied by DSC. Parts a and b of Figure 1 show the cooling and heating DSC thermograms of AN05CL03 and PCL homopolymer, respectively. As shown, the glass transition of PAN block in AN05CL03 can be clearly identified at ca. 102 °C, and the T_g value is consistent with the T_g of homopolymer according to the synthesized molecular weight (i.e., $T_{g,PAN}$ with M_n of 15 000 g/mol at about 135 °C from our results), suggesting that microphase-separated PAN microdomains might be formed from the melt state. Also, the

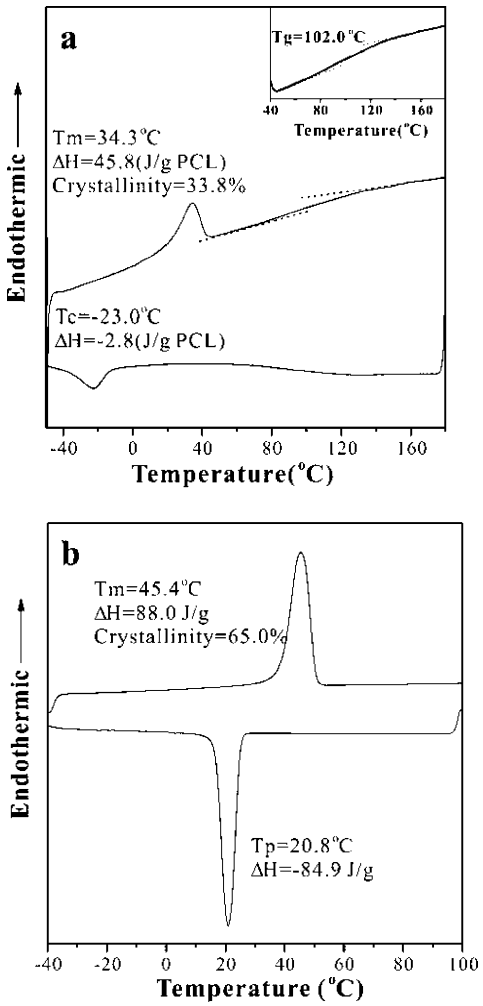

Figure 1. DSC thermograms of (a) AN05CL03 block copolymer and (b) homopolymer PCL. Inset of (a) shows the T_g of PAN block in AN05CL03.

thermogram of AN05CL03 exhibits an exothermic peak at −23 °C while that for PCL homopolymer at 20.8 °C. The significant decrease in the maximum crystallization temperature indicates that PCL blocks are certainly crystallized within confined environment.[37−39] On the basis of the solubility parameters of $\delta_{PAN} = 14.1\ (cal/cm^3)^{1/2}$ and $\delta_{PCL} = 9.2\ (cal/cm^3)^{1/2}$,[40,41] strongly segregated microdomains are expected in the temperature ranges studied.

Namely, strongly segregated microdomains can be formed in PAN−PCL at which microphase-separated morphology is preserved after PCL crystallization in-between vitrified PAN microdomains. To further identify the morphology of PAN−PCLs, microsections of quenched PAN−PCL samples (referred as pristine samples) at room temperature were examined by TEM. Owing to the RuO_4 staining effect, PAN and PCL microdomains appeared as dark and bright regions, respectively. As observed, the TEM image of AN05CL03 ($f_{PAN}{}^v = 0.6$) (Figure 2a) exhibited typical microphase-separated lamellar morphology with *d*-spacing measured at around 14 nm. Consistent with the thermal analysis, lamellar nanostructure can be preserved after the assumed thermal treatment regardless of PCL crystallization. Corresponding SAXS results (Figure 2b) further confirm the observed lamellar nanostructure where the scattering peaks occur at q^* ratio of 1:2 and the *d*-spacing is determined as 16 nm. The broad second peak is attributed to the PCL crystalline leading to much significant electron density variation from PAN and amorphous PCL.[42,43] Consequently, the broad-

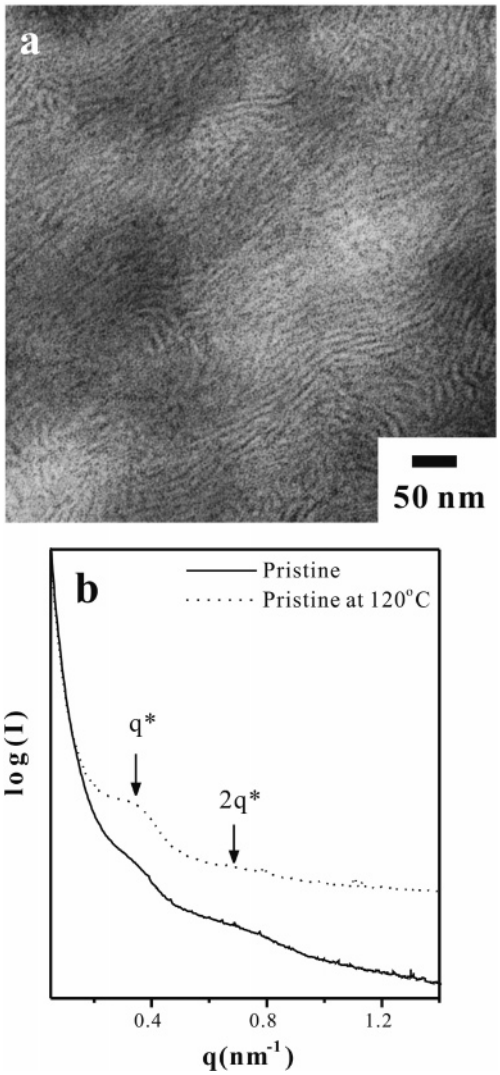

Figure 2. (a) TEM micrograph of pristine AN05CL03 ($f_{PAN^{v}} = 0.6$) and (b) corresponding 1D SAXS profiles examined at room temperature and 120 °C.

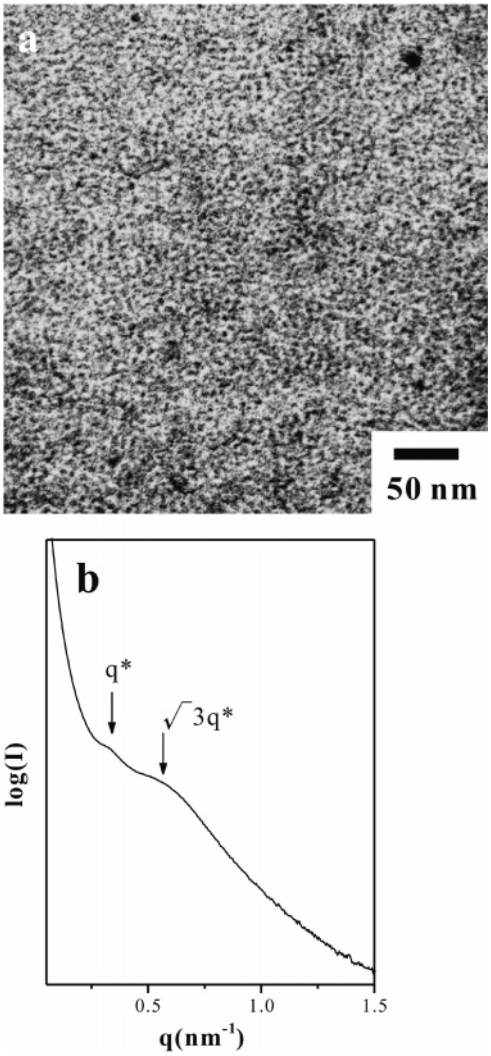

Figure 3. (a) TEM micrograph of pristine AN03CL05 ($f_{PAN^{v}} = 0.33$) and (b) corresponding 1D SAXS profile examined at room temperature.

ness of the peak becomes narrow as examined at temperature above T_m of PCL blocks (dotted line of Figure 2b). Similar results for the structure identification of various PAN−PCL samples were also obtained. For instance, a hexagonal cylindrical structure for AN03CL05 ($f_{PAN^{v}} = 0.33$) was observed by TEM (Figure 3) at which scattering peaks occurred at q^* ratio of $1:\sqrt{3}$ in SAXS can be identified. Consequently, various PAN−PCL samples having nanostructures such as hexagonal cylinder and lamellar morphology were prepared. To produce large amounts of porosity (i.e., higher volume fraction of dispersive PCL component), lamellar nanostructure was chosen as the templates for the preparation of mesoporous carbons instead of the PAN cylinder nanostructure in this study.

Stabilization of PAN−PCL Block Copolymers. One indispensable process for carbonization of PAN is stabilization, a process well-known in the field of carbon fibers, achieved through specific thermal treatment. The stabilization process of PAN precursor fibers involves low-temperature heating (200−300 °C) of the fiber to transform them into a structure that can be subjected to high-temperature carbonization treatment without melting or fusion of the fibers. The unsaturated side groups (nitrile groups) in the linear polymer of PAN undergo a polymerization reaction on heating, then form a cyclized structure known as a ladder structure, and finally become a cross-linked network. The cyclized structure is stable toward heat and can be converted to turbostatic carbon on subsequent carbonization at high temperatures (∼1000−2000 °C) in an inert atmosphere (i.e., in nitrogen atmosphere) or vacuum.[17−21] To achieve efficient processes for stabilization, thermal analyses were carried out by using DSC and TGA. As shown in Figure 4, the TGA thermogram and corresponding trace of weight loss rate in air revealed that stabilization reaction of PAN block in copolymers occurs at ca. 300 °C (first significant weight loss). Followed by the stabilization, PCL blocks were thermally degraded at about 400 °C (second weight loss with ca. 40 wt %, approximately equal to the constituent composition of PCL), whereas oxidative degradation reaction of stabilized PAN blocks occurred at about 600 °C. Finally, the carbonized samples can be further oxidized to completely degenerate the residual weight because of the oxygen-contained environment. Consistent with the TGA results, the DSC thermogram in air showed a large exothermic peak due to stabilization reaction where the onset temperature and the peak temperature were at 230 and 302 °C, respectively. The second exothermic peak is attributed to the thermal degradation of PCL block. The further signal of thermal degradation is not available in DSC because of the limited temperature of DSC used. As a result, a reasonable temperature for stabilization (230 °C) was thus chosen. The IR spectra of pristine and stabilized PAN block copolymers are shown in Figure 5. The FTIR spectrum taken prior to thermal

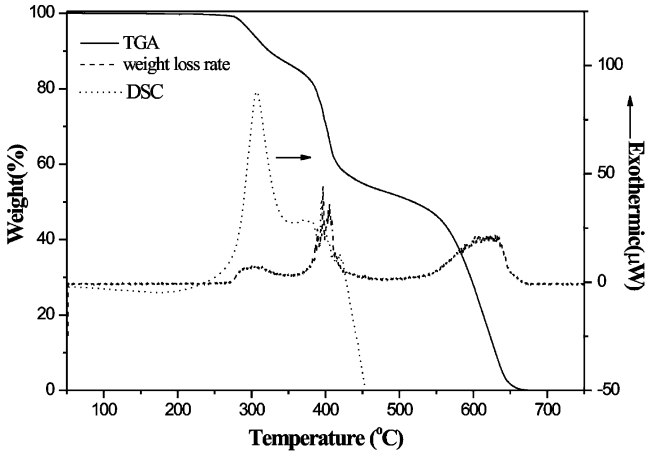

Figure 4. TGA and DSC thermograms of pristine AN05CL03 profiles scanned at 10 °C/min heating in air. The trace of weight loss rate is the differential term of TGA thermogram by temperature.

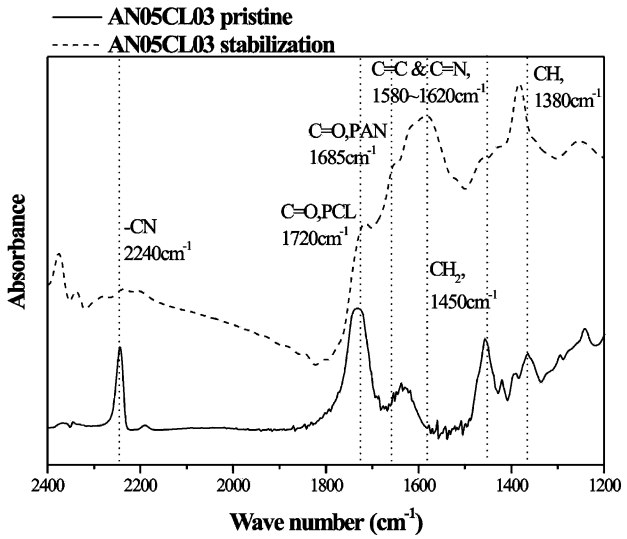

Figure 5. FTIR spectra of pristine and stabilized AN05CL03. The stabilized samples were heated at 230 °C for 20 h in atmosphere.

treatment showed a characteristic strong absorption band at ~2240 cm^{-1}, which corresponds to a CN group of the PAN component. The strong and broad absorption bands between 1580 and 1620 cm^{-1} indicated the formation of C═C and C═N bonds derived from the cyclization and cross-linking reaction involving CN groups. The intensity of the absorption bands attributed to CN groups thus gradually diminished due to the formation of C═N bonds. Also, the intensity of CH_2 groups (1450 cm^{-1}) on PAN component decreased and the intensity of CH groups (1380 cm^{-1}) increased slightly due to the oxidation of PAN backbone and formation of ladder structure. The shoulder adsorption band at 1685 cm^{-1}, corresponding to C═O bond of PAN component, indicated the oxidation of PAN component during stabilization. As a result, oxidation of PAN backbone occurred, and eventually cyclization reaction (namely, the formation of cyclic and aromatic structures) was formed, whereas no significant change on PCL block (i.e., strong absorption band at ~1720 cm^{-1}) was involved after stabilization. Since this stabilization reaction is a dramatic exothermic response, whether or not the intrinsic nanostructure remains is critical for templation. The formed morphology after stabilization was thus examined by TEM and SAXS. As shown (Figure 6a), the samples retain the intrinsic microphase-separated texture even though the *d*-spacing becomes larger (ca. 17 nm). The preserved nanostructure was further identified by SAXS (Figure

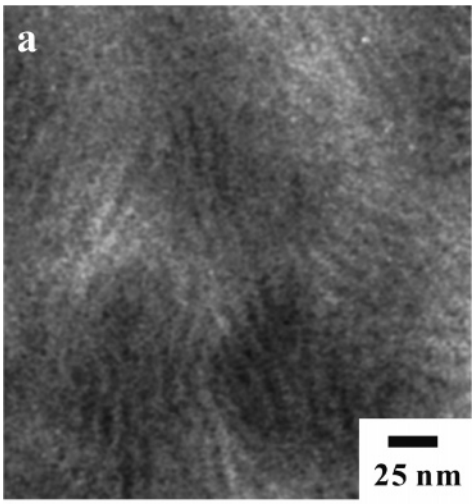

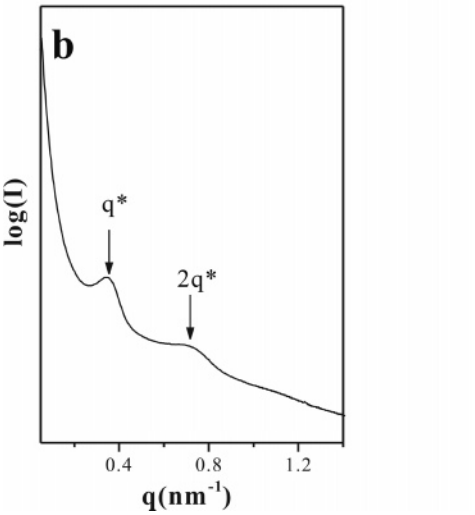

Figure 6. (a) TEM micrograph and (b) 1D SAXS profile of stabilized AN05CL03. The stabilized samples were heated at 230 °C for 20 h in atmosphere.

6b) where the scattering peaks were found to occur at *q** ratio of 1:2, and the *d*-spacing was determined as 20 nm from the primary peak, in good agreement with the TEM results. The domain spacing increased from 16 to 20 nm according to the SAXS results, whereas the domain spacing increased from 14 to 17 nm as observed by TEM. The expected change might be attributed to the formation of ladder structure resulting from chain stretching during stabilization.[44]

Degradation of PCL in PAN−PCL. As evidenced by thermal analysis, the stabilization process can be achieved by thermal treatment in air, but continuous heating under air environment may cause the complete degradation of stabilized PAN−PCL. So, the stabilized PAN−PCL samples should be treated in inert environment (i.e., in nitrogen) so as to form the scaffold for mesoporous carbon materials from the PAN−PCL templates. To create the mesoporous templates, the stabilized PAN−PCL samples were gradually heated to high temperature in nitrogen. It is noted that the complete removal of the PCL component can be achieved by heating the homopolymer from 50 to 750 °C in nitrogen, as evidenced by TGA with a weight loss larger than 99% at 450 °C. Also, the stabilized PAN component was not affected by thermal degradation of the PCL component. Figure 7a shows the TEM morphology of mesoporous PAN after the complete degradation of the PCL component. The electron density contrast was greatly enhanced due to the formed porous texture so that the morphology can

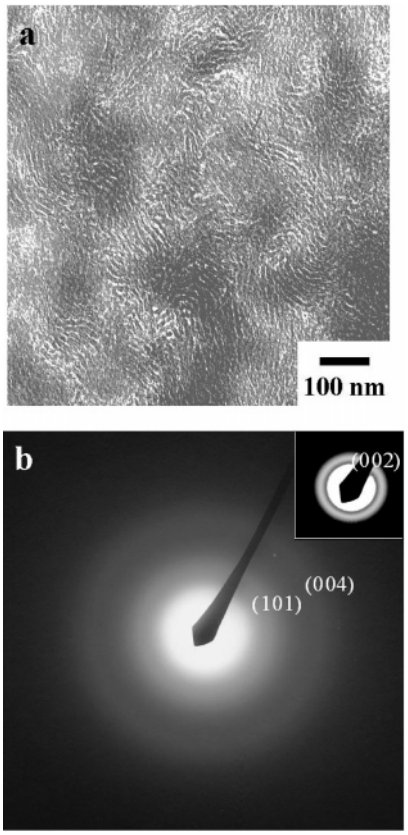

Figure 7. (a) TEM phase image and (b) ED pattern of AN05CL03 stabilized at 230 °C for 20 h in atmosphere and then thermally degraded PCL block at 450 °C under nitrogen. The dark region of TEM micrograph was PAN block. Inset of ED pattern showed the inner diffraction, and the ED pattern is similar to the results of carbon fibers.

be clearly observed without staining. Randomly distributed porous texture originating from degraded PCL lamellar texture was observed. Furthermore, the *d*-spacing was determined to be identical to the stabilized sample, further confirming the preserved nanostructure from the templates. We speculate that similar results should also be expected by hydrolysis of PCL using alkaline solution such as a sodium hydroxide solution of methanol/water or a potassium hydroxide and CETAB solution of methanol/water. Nevertheless, it is noted that the nitrile groups of PAN block could also be hydrolyzed in alkaline condition.[45] Consequently, the PAN-containing block copolymers were stabilized before PCL hydrolysis in this study. As mentioned in Experimental Section, it is not practical to carry out the hydrolytic process for the preparation of mesoporous carbon precursors by using sodium hydroxide solution due to the extremely long hydrolytic process for PCL degeneration. To improve the hydrolytic efficiency, the potassium hydroxide and CETAB solution of methanol/water was used. Nevertheless, the PAN component was also etched out by the hydrolysis solution due to the strong basicity of the potassium hydroxide even with stabilization, resulting in porous microstructures having disorder-like textures. It is expected to achieve optimal hydrolysis condition for the formation of mesoporous microstructures with preserved textures by using tuning hydrolysis solution for stabilized PAN; the approach for the best etching condition is still in progress.

To examine the crystalline structure of formed scaffold after PCL thermal degradation, the ED pattern was obtained from the microsection of the scaffold (Figure 7b). Similar to the diffraction results of carbon fibers,[18] the primary reflection of (002) (corresponding to a spacing of *d*-spacing = 3.45 Å), a weak reflection of (101) which may overlap the reflection of (100) and a diffuse reflection of (004) can be resolved. Also, a ring pattern, reflection of randomly oriented lamellar nanostructure, was obtained as expected. The mesoporous scaffold was further examined by FESEM (Figure 8) where the size of pores attributed to the degradation of PCL is roughly equivalent to the bright regions in the TEM micrographs. As a result, the nanostructure of the PAN−PCL system might be preserved after the thermal degradation of PCL so as to create carbonized scaffold due to the templation of microphase-separated PAN−PCL.

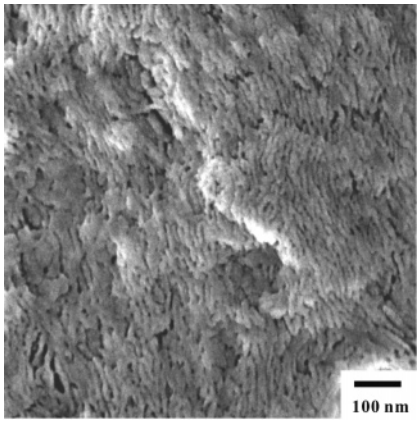

Figure 8. FESEM topographic image of AN05CL03 stabilized at 230 °C for 20 h in atmosphere and then thermally degraded PCL block at 450 °C under nitrogen.

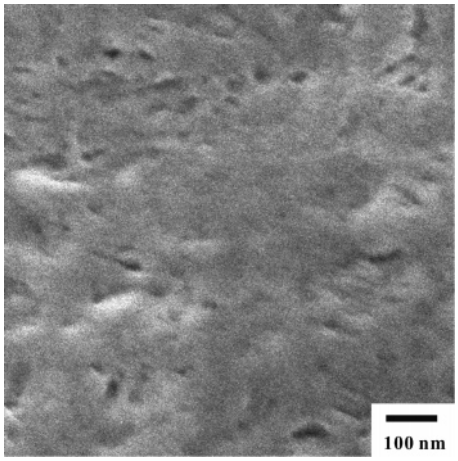

Figure 9. FESEM morphology of carbonized AN05CL03 stabilized at 230 °C for 20 h in atmosphere and then carbonized at 800 °C.

Carbonization of Mesoporous PAN. To complete the carbonization of the mesoporous scaffolds, the stabilized samples were further heated to 800 °C with an extremely slow ramp rate, 1 °C/min. After high-temperature treatment for carbonization, the topographic morphology was observed by FESEM (Figure 9). The lamellar nanostructure with regular texture degenerated, but a random-sized porous structure with broad pore size range was found. The disordered nanostructures after carbonization might be attributed to the collapse of stabilized PAN blocks in the process of high-temperature thermal treatment regardless of the formation of highly cross-linked PAN; the CN groups of PAN transformed into C=N bonding upon stabilization as observed by FTIR (Figure 5). The progress of carbonization of PAN block copolymer was monitored with SAXS and WAXD. While at high-temperature thermal treatment, a broad bump in the SAXS profile (Figure 10a) can be clearly identified. The diffused scattering result might be attributed to the

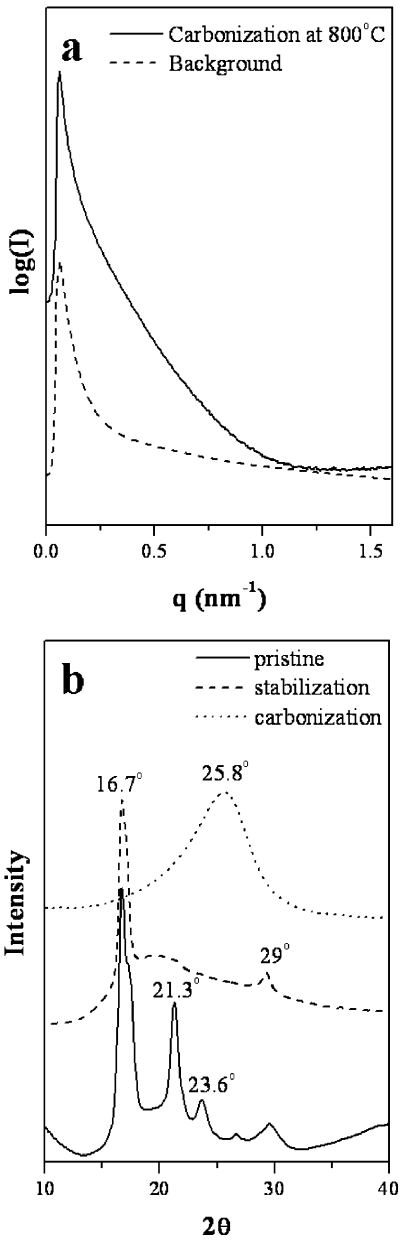

Figure 10. (a) SAXS profiles of carbonized AN05CL03 and background. (b) WAXD profiles of each step of carbonization procedure.

formation of large amounts of random-oriented pores in the carbon matrix, as shown in Figure 9.[46] Figure 10b is the comparison of wide-angle X-ray diffraction patterns observed for pristine, stabilized, and carbonized samples at room temperature from $2\theta = 10°$ to 40°. The main reflection of pristine PAN−PCL in the WAXD pattern was at $2\theta = 16.7°$, corresponding to PAN which was similar to PAN fiber precursor, and a weak reflection at $2\theta = 29°$ as well.[15] PCL blocks showed two strong reflections at $2\theta = 21.3$ and 23.6°. Upon stabilization, the reflections of PAN component at $2\theta = 16.7°$ and 29° became sharper and stronger due to the improvement in the orientation under dimensional constraints so as to lead the perfection of the molecular chain packing. Also, the reflections of crystalline PCL blocks disappeared in the profile of stabilized PAN−PCL due to some thermal degradation at such high temperature, even though PCL blocks had not been thermal-degraded completely. After carbonization, a broad peak centered at $2\theta = 25.8°$, which corresponded to the interplanar spacing of 0.36 nm, developed. The peaks could be identified as (002) spacing of a graphitic carbon structure.

Confinement Effect on Carbonization. It is well-known that the degree of stretching and the orientation of PAN molecules are critical to the formation of carbonized fibers. A large degree of PAN chain scission may occur due to the lack of chain stretching and orientation so that a random-oriented PAN homopolymer is mostly vaporized after carbonization for nonstretching samples, namely brittle failure mechanism.[17,47] On the basis of interfacial energy consideration, molecular chains in microphase-separated domains cannot be random coils, but stretching chains due to a simple manner by balancing the free energy associated with the interface between the microdomains against the energy associated with the stretching of the chains away from the interface.[48,49] In contrast to disordered phase at which the characteristic length scaling factor is $N^{1/2}$, the characteristic length scaling factor increases with microphase separation (say $N^{2/3}$ for strong segregation limits). We speculate that the molecular chains of PAN within microphase-separated microdomains should form stretched conformation due to the thermodynamic consideration of the immiscibility of each blocks. Consequently, the carbonization of PAN in the microphase-separated nanostructures may occur from the stretched chain condition so as to avoid the induction of PAN chain scission in large degree.

Conclusions

PAN−PCL is a new nanocarbon precursor system in which PAN block is the carbonization precursor and PCL block is the degradable component. The nanostructures of PAN−PCLs were identified by TEM and SAXS results. The stabilization condition of PAN block copolymer was identified by thermal analysis, and the stabilized nanostructure was identical to intrinsic texture. PCL blocks can be thermally degraded without involving the change on nanostructure. In contrast to the preservation of nanostructure after thermal degradation of PCL, the hydrolytic process for PCL component may cause the change of intrinsic nanostructures due to the simultaneous etching of PAN and PCL components during hydrolysis. Systematic study with respect to the achievement of optimal condition for hydrolysis should be carried out in order to preserve the templated nanostructure after hydrolysis. Also, significant change on the self-assembled nanostructures was found after carbonization at which the templated nanostructures may vary due to the collapse of mesoporous matrix. We thus expect that the mesoporous carbon scaffolds can thus be manufactured from carbonization of bulk PAN templates once optimal conditions for carbonization can be achieved. Consequently, the self-assembly PAN−PCL materials may give rise to a promising and convenient way for the manufacturing of mesoporous carbon.

Acknowledgment. The financial support of the National Science Council (Grant NSC 93-2216-E-007-010) is acknowledged. We thank Dr. B. S. Hsiao of the Chemistry Department, State University of New York at Stony Brook, and Drs. I. Sics, C. A. Avila-Orta, and L. Rong, of the National Synchrotron Light Source at Brookhaven National Laboratory, and Drs. U.-S. Jeng and Y.-S. Sun of the National Synchrotron Radiation Research Center for their help in Synchrotron SAXS experiments. We also thank Ms. P.-C. Chao, Ms. Y.-C. Lin, and Mr. Y.-F. Lu of Regional Instruments Center at NCHU for their help in TEM and FESEM experiments.

References and Notes

(1) Bansal, C. R.; Donnet, J.-B.; Stoeckli, F. *Active Carbon*; Marcel Dekker: New York, 1988.

(2) Foley, H. C. *Microporous Mater.* **1995**, *4*, 407−433.
(3) Han, B.-H.; Zhou, W.; Sayari, A. *J. Am. Chem. Soc.* **2003**, *125*, 3444−3445.
(4) Yoon, S. B.; Kim, J. Y.; Yu, J.-S. *Chem. Commun.* **2001**, *6*, 559−560.
(5) Joo, S. H.; Choi, S. J.; Oh, I.; Kwak, J.; Liu, Z.; Terasaki, O.; Ryoo, R. *Nature (London)* **2001**, *412*, 169−172.
(6) Ryoo, R.; Joo, S. H.; Kruk, M.; Jaroniec, M. *Adv. Mater.* **2001**, *13*, 677−681.
(7) Lee, J.; Yoon, S.; Hyeon, T.; Oh, S. M.; Kim, K. B. *Chem. Commun.* **1999**, *21*, 2177−2178.
(8) Han, S. J.; Sohn, K.; Hyeon, T. *Chem. Mater.* **2000**, *12*, 3337−3341.
(9) Han, S. J.; Kim, M.; Hyeon, T. *Carbon* **2003**, *41*, 1525−1532.
(10) Lu, A. H.; Kiefer, A.; Schmidt, W.; Schuth, F. *Chem. Mater.* **2004**, *16*, 100−103.
(11) Xia, Y. D.; Yang, Z. X.; Mokaya, R. *Chem. Mater.* **2006**, *18*, 140−148.
(12) Ma, Z. X.; Kyotani, T.; Liu, Z.; Terasaki, O.; Tomita, A. *Chem. Mater.* **2001**, *13*, 4413−4415.
(13) Lee, J.; Yoon, S.; Oh, S. M.; Shin, C. H.; Hyeon, T. *Adv. Mater.* **2000**, *12*, 359−362.
(14) Kruk, M.; Jaroniec, M.; Ryoo, R.; Joo, S. H. *J. Phys. Chem. B* **2000**, *104*, 7960−7968.
(15) Kim, T.-W.; Park, I.-S.; Ryoo, R. *Angew. Chem., Int. Ed.* **2003**, *42*, 4375−4379.
(16) Sonobe, N.; Kyotani, T.; Tomita, A. *Carbon* **1988**, *26*, 573−578.
(17) Edie, D. D. *Carbon* **1988**, *36*, 345−362.
(18) Bajaj, P.; Roopanwal, A. K. *Rev. Macromol. Chem. Phys.* **1997**, *C37*, 97−147.
(19) Henrici-Olive, G.; Olive, S. *Adv. Polym. Sci.* **1983**, *51*, 1−60.
(20) Overberger, C. G.; Moore, J. A. *Adv. Polym. Sci.* **1970**, *7*, 113−150.
(21) Xue, T. J.; McKinney, M. A.; Wilkie, C. A. *Polym. Degrad. Stab.* **1997**, *58*, 193−202.
(22) Kowalewski, T.; Tsarevsky, N. V.; Matyjaszewski, K. *J. Am. Chem. Soc.* **2002**, *124*, 10632−10633.
(23) Kowalewski, T.; McCullough, R. D.; Matyjaszewski, K. *Eur. Phys. J. E* **2003**, *10*, 5−16.
(24) Tang, C. B.; Tracz, A.; Kruk, M.; Zhang, R.; Smilgies, D. M.; Matyjaszewski, K.; Kowalewski, T. *J. Am. Chem. Soc.* **2005**, *127*, 6918−6919.
(25) Tang, C. B.; Qi, K.; Wooley, K. L.; Matyjaszewski, K.; Kowalewski, T. *Angew. Chem., Int. Ed.* **2004**, *43*, 2783−2787.
(26) Leiston-Belanger, J. M.; Penelle, J.; Russell, T. P. *Macromolecules* **2006**, *39*, 1766−1770.
(27) Kruk, M.; Dufour, B.; Celer, E. B.; Kowalewski, T.; Jaroniec, M.; Matyjaszewski, K. *Chem. Mater.* **2006**, *18*, 1417−1424.
(28) Liang, C. D.; Hong, K. L.; Guiochon, G. A.; Mays, J. W.; Dai, S. *Angew. Chem., Int. Ed.* **2004**, *43*, 5785−5789.
(29) Zalusky, A. S.; Olayo-Valles, R.; Taylor, C. J.; Hillmyer, M. A. *J. Am. Chem. Soc.* **2001**, *123*, 1519−1520.
(30) Zalusky, A. S.; Olayo-Valles, R.; Wolf, J. H.; Hillmyer, M. A. *J. Am. Chem. Soc.* **2002**, *124*, 12761−12773.
(31) Leiston-Belanger, J. M.; Russell, T. P.; Drockenmuller, E.; Hawker, C. J. *Macromolecules* **2005**, *38*, 7676−7683.
(32) Ho, R.-M.; Chiang, Y.-W.; Tsai, C.-C.; Lin, C.-C.; Ko, B.-T.; Huang, B.-H. *J. Am. Chem. Soc.* **2004**, *126*, 2704−2705.
(33) Ho, R.-M.; Tseng, W.-H.; Fan, H.-W.; Chiang, Y.-W.; Lin, C.-C.; Ko, B.-T.; Huang, B.-H. *Polymer* **2005**, *46*, 9362−9377.
(34) Liu, Y.-C.; Ko, B.-T.; Lin, C.-C. *Macromolecules* **2001**, *34*, 6196−6201.
(35) Pierce, M. E.; Harris, G. D.; Islam, Q.; Radesca, L. A.; Storace, L.; Waltermire, R. E.; Wat, E.; Jadhav, P. K.; Emmett, G. C. *J. Org. Chem.* **1996**, *61*, 444−450.
(36) Shabana, H. M.; Olley, R. H.; Bassett, D. C.; Jungnickel, B.-J. *Polymer* **2000**, *41*, 5513−5523.
(37) Chen, H.-L.; Hsiao, S.-C.; Lin, T.-L.; Yamauchi, K.; Hasegawa, H.; Hashimoto, T. *Macromolecules* **2001**, *34*, 671−674.
(38) Loo, Y. L.; Register, R. A.; Ryan, A. J. *Phys. Rev. Lett.* **2000**, *84*, 4120−4123.
(39) Huang, P.; Zhu, L.; Guo, Y.; Ge, Q.; Jing, A. J.; Chen, W. Y.; Quirk, R. P.; Cheng, S. Z. D.; Thomas, E. L.; Lotz, B.; Hsiao, B. S.; Avila-Orta, C. A.; Sics, I. *Macromolecules* **2004**, *37*, 3689−3698.
(40) Brandrup, J.; Immergut, E. H. *Polymer Handbook*, 3rd ed.; Wiley-Interscience: New York, 1989.
(41) Meaurio, E.; Zuza, E.; Sarasua, J. R. *Macromolecules* **2005**, *38*, 9221−9228.
(42) Ryan, A. J.; Hamley, I. W.; Bras, W.; Bates, F. S. *Macromolecules* **1995**, *28*, 3860−3868.
(43) Verma, R.; Marand, H.; Hsiao, B. S. *Macromolecules* **1996**, *29*, 7767−7775.
(44) Gupta, A.; Harrison, I. R. *Carbon* **1996**, *11*, 1427−1445.
(45) Riqueza, E. C.; de Aguiar, A. P.; Aguiar, M. R. M. P.; Maria, L. C. D. *Polym. Bull. (Berlin)* **2005**, *55*, 31−40.
(46) Kaburagi, M.; Bin, Y. Z.; Zhu, D.; Xu, C. Y.; Matsuo, M. *Carbon* **2003**, *41*, 915−926.
(47) Johnson, D. J. *J. Phys. D: Appl. Phys.* **1987**, *20*, 287−291.
(48) Shull, K. R. *Macromolecules* **1992**, *25*, 2122−2133.
(49) Matsen, M. W.; Bates, F. S. *Macromolecules* **1996**, *29*, 1091−1098.

MA062798Y